ACS Catalysis

Viewpoint

pubs.acs.org/acscatalysis

Reporting of Reactivity for Heterogeneous Photocatalysis

Israel E. Wachs,* Somphonh P. Phivilay, and Charles A. Roberts†

Operando Molecular Spectroscopy & Catalysis Laboratory, Department of Chemical Engineering, Lehigh University, Bethlehem, Pennsylvania 18015, United States

The absence of standardization in both the measurement and the reporting of heterogeneous photocatalysis reactivity data has prevented quantitative comparisons between different photocatalysts and advances in fundamental understanding of the photocatalysis reaction, respectively. The call for adoption of a standard photocatalysis measurement procedure, to prevent masking of the photocatalysis reactivity by saturation of light absorption or mass transfer effects, was recently proposed to allow ranking of different photocatalysts for their performance and comparison of reactivity reported from different laboratories.[1,2] Adoption of the standardized measurement protocols by photocatalysis researchers is indeed critical for advancing the heterogeneous photocatalysis field. Standardized reactivity measurement, however, still does not address fundamental aspects of the photocatalysis process (e.g., structure−activity relationships), which would require normalizing the reactivity per number of surface photocatalytic active sites as is practiced for heterogeneous catalysis.[1]

Most heterogeneous photocatalysis publications report the photocatalyst performance as mass normalized Turnover Rate (TOR_m: moles converted or produced per gram of photocatalyst per unit of time), as a consequence of the ease of determining the number of product moles formed, most commonly by chromatography, and simply weighing the mass of the employed photocatalyst. This viewpoint (i) examines the pros and cons of various methods in reporting photocatalysis reactivity (TOR_m, TOR_s (molecules converted or produced per m^2 of photocatalyst per unit time), and TOF (moles converted or produced per photoactive surface site of photocatalyst per unit time)), (ii) shows how TOF can be determined for heterogeneous photocatalysts from surface characterization methods that provide the number of photoactive surface sites per gram (N_s) of photocatalysts, and (iii) demonstrates how fundamental photocatalytic structure−reactivity relationships can be determined by using the TOR_s and TOF methodologies to report photocatalysis reactivity.[3,4]

An examination of the heterogeneous photocatalysis literature reveals that multiple expressions are in use to report photocatalytic reactivity. The term photonic efficiency (PE), formerly referred to as Apparent Quantum Efficiency (AQE), is the initial rate of the photoreaction to the rate of incident photons inside the irradiation window of the reactor under a set of well described conditions.[5,6] This term is an *apparent* efficiency since it depends on the incident photons and not the photons absorbed by the photocatalyst. The intrinsic photocatalytic activity is termed quantum efficiency and is the initial rate of the photoreaction divided by the rate of photons absorbed by the photocatalyst at a set of well described conditions.[5,6] Quantum efficiency reflects the overall intrinsic efficiency of a photocatalyst in harnessing the photons absorbed to generate excited electrons and holes that diffuse to the surface to participate in the photocatalytic chemical reaction.[5,6] The difficulty associated with the measurement of quantum efficiency for heterogeneous photocatalysts has favored the use of the easier to measure PE of heterogeneous photocatalysts. PE is useful for comparison of photocatalytic reactivity under the same illumination conditions.

Heterogeneous photocatalysis is a complex process since both the photocatalyst bulk lattice and the surface sites contribute to the overall photocatalytic process. The function of the bulk lattice is to absorb the incident photons and generate excited electrons and holes. The function of the surface catalytic active sites is to harness the excited electrons and holes reaching the surface to perform the catalytic reaction (chemical transformation). Although quantum efficiency and even PE of a photocatalyst parameters describe how well a photocatalyst functions for a given reaction at a set of well described conditions, they do not provide any fundamental insights about the individual contributions of the photocatalyst bulk lattice (e.g., particle size, crystallinity, etc.) or photoactive surface sites (e.g., surface area, number of exposed photoactive sites, surface structure, etc.) to the overall photocatalysis process. The current common practice of normalizing photocatalytic productivity per gram of a photocatalyst per unit time informs about the effectiveness of a photocatalyst per unit mass, which may have practical merit, but does not relate photocatalysis performance to possible bulk and surface changes in the characteristics of the photocatalyst bulk lattice and surface catalytic active sites.

For example, altering the heterogeneous photocatalyst surface area affects the number of exposed photoactive surface sites[3,4] or altering the photocatalyst bulk lattice crystallinity (increasing crystal order and decreasing number of bulk defects) can affect photon absorption and decrease the number of undesirable trap sites that recombine excited electrons/holes and prevent them from reaching the surface to participate in the photocatalytic chemical reaction. By analogy to traditional heterogeneous catalysis, there are many advantages that result from the use of a specific reactivity parameter and its nomenclature such as Turnover Frequency (TOF), which is a specific reactivity parameter per exposed active surface site per unit time for a heterogeneous catalyst.[7] By normalizing the photocatalytic productivity per number of surface sites, (TOR_s), or even the specific TOF when the number of photoactive surface sites are known, allows for better understanding of bulk and surface photocatalyst structural variations. In other words, TOR_s and TOF photoactivity values would be structure sensitive to both crystallinity of the bulk

Received: July 24, 2013
Published: October 3, 2013

dx.doi.org/10.1021/cs4005979 | ACS Catal. 2013, 3, 2606−2611

lattice (affecting efficiency of absorption of photons and number of e^-/h^+ traps) and surface features (surface composition and possible preferential exposure of specific surface facets possessing unique photoactivity).[5]

Several examples are given below for determining photocatalytic TOF and TOR_s values and how using TOF and TOR_s to express photocatalyst productivity improves our fundamental understanding of photocatalytic materials and the bulk and surface factors affecting heterogeneous photocatalysis.

Single Component Mono-Phasic Heterogeneous Photocatalysts. A single component monophasic photocatalyst consists of a single bulk phase (e.g., TiO_2, GaN, etc.) and is schematically shown in Figure 1 for photocatalytic

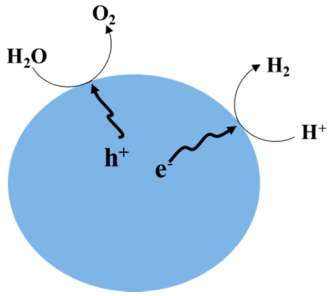

Figure 1. Schematic of single component monophasic heterogeneous photocatalyst for photocatalytic splitting of water.

splitting of water. The high photo-oxidation activity of UV-illuminated (>290 nm) TiO_2 particles for oxidation of undesirable organics in air and water has motivated many photocatalytic studies by TiO_2 as a function of particle size.[3,4,8,9] Typically, both the particle dimension and the bulk lattice crystallinity of a series of TiO_2 catalysts are altered by calcining the starting titania material at higher temperatures.[3,4,8,9] Such thermal treatments can be used to study the effects of particle dimension and/or bulk lattice crystallinity on photoactivity for a family of catalysts. In the case of TiO_2 photo-oxidation of the organic molecule cyclohexane to cyclohexanone, normalization of the cyclohexane to cyclohexanone photocatalysis as TOR_m generally leads to an apparent decrease in photoactivity with increasing particle dimension (7−30 nm).[3,4] Normalization of the cyclohexane to cyclohexanone photocatalytic activity per surface parameter, such as surface area or number of surface hydroxyls (OH), however, gives rise to an increase in photoactivity TOR_s with increasing particle diameter for the *same photocatalyst system data*.[3,4]

How to reconcile such quite different photoactivity trends obtained for TOR_m and TOR_s for the same photocatalysts and photoreaction? Just from the mass normalized TOR_m definition, the origin of the decrease in photoactivity is not apparent. Of course, the decrease is dominated by the decrease in number of surface sites as the particles become larger. The increase in the surface normalized TOR_s with particle diameter, however, reflects a structural change of the TiO_2 photocatalyst since this parameter accounts for the changing number of photoactive surface sites. Complementary characterization studies demonstrated that the increase in the photocatalytic TOR_s is related to enhanced bulk crystallinity of TiO_2 that increases the number and lifetime of excited e^-/h^+ pairs in the bulk lattice that will be able to reach the surface.[3,4] The increase in the photocatalytic TOR_s, specific TOF when normalized per surface OH groups, is only a factor of ∼3 with increasing particle size, which also reveals that the bulk lattice characteristics of TiO_2 NPs employed in this study exert only a small effect on the overall photocatalytic process. This example nicely demonstrates that when a family of photocatalysts undergoes large surface area changes it is important to account for the changing Brunauer−Emmett−Teller (BET) values as TOR_s, or specific TOF when N_s is known, to be able to extract the fundamental influence of bulk lattice structural changes upon the photoactivity.

Multicomponent Mono-Phasic Heterogeneous Photocatalysts. A multicomponent monophasic photocatalyst consists of a single bulk phase (e.g., TaON, $[(GaN)_{1-x}(ZnO)_x]$, $NaTaO_3$, etc.) consisting of more than 2 elements. Promoted $NaTaO_3$ photocatalysts have been found to be the most active materials for photocatalytic splitting of H_2O to H_2 and O_2 with UV excitation (>270 nm).[10,11] The addition of La_2O_3 during the catalyst synthesis was found to increase TOR_m by a factor of ∼3 and TEM images exhibited the formation of smaller particles containing ordered stepped surfaces. It was proposed that the enhanced TOR_m photoactivity was related to the accumulation of the La_2O_3 electronic promoter at the surface steps of $NaTaO_3$, but other researchers found the steps transfer electrons less efficiently compared to $NaTaO_3$.[12] A closer examination of the photoactivity rate in terms of TOR_s, however, reveals that the surface normalized TOR_s actually decreases by a factor of ∼3 upon the addition of the La_2O_3 promoter to $NaTaO_3$. The disparity between these two ways of looking at the reactivity, TOR_m vs TOR_s, of this photocatalyst system is related to the increase in surface area, by a factor of ∼7, resulting from the addition of La_2O_3 promoter to the synthesis of $NaTaO_3$ that is not reflected in the TOR_m rate. It, thus, appears that La_2O_3 is just a textural promoter that increased the $NaTaO_3$ surface area and the number of available photoactive surface sites, by stabilizing smaller $NaTaO_3$ particles. The highly crystalline $NaTaO_3$ bulk lattice was not significantly perturbed by the introduction of La_2O_3 (reflected by its same Raman spectrum and UV−vis band gap). Furthermore, the decrease of ∼3 in TOR_s from the introduction of the La_2O_3 promoter indicates that the formation of the stepped surfaces for the La-promoted $NaTaO_3$ photocatalyst does not enhance the specific photoactivity TOR_s. The decrease in TOR_s is most probably related to the surface La_2O_3 sites that are actually inactive photocatalytic sites that cover the photoactive surface sites of $NaTaO_3$ (as surface analysis reveals below, La_2O_3 is surface segregated on $NaTaO_3$). Thus, the role of the La_2O_3 promoter appears to be that of a textural promoter and not an electronic promoter. This example again shows that when a family of photocatalysts undergoes large surface area changes it is important to account for the changing BET values as TOR_s to be able to extract the fundamental influence of surface changes upon the photoactivity.

Biphasic Heterogeneous Photocatalysts. Biphasic heterogeneous photocatalysts consist of two different phases, and each phase may either be single- or multicomponent (e.g., supported $Rh_{2-y}Cr_yO_3/[(GaN)_{1-x}(ZnO)_x]$, supported $NiO/NaTaO_3$ with NiO NPs at high Ni loadings, etc.) as depicted in Figure 2 for photocatalytic splitting of water. The supported $Rh_{2-y}Cr_yO_3/[(GaN)_{1-x}(ZnO)_x]$ system is the most active photocatalyst found to date for splitting of water with visible light excitation (>420 nm).[13,14] In the absence of the $Rh_{2-y}Cr_yO_3$ nanoparticles (NPs), the $[(GaN)_{1-x}(ZnO)_x]$

dx.doi.org/10.1021/cs4005979 | ACS Catal. 2013, 3, 2606−2611

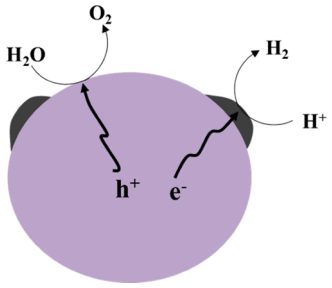

Figure 2. Schematic of biphasic heterogeneous photocatalysts for photocatalytic splitting of water. Purple, $[(GaN)_{1-x}(ZnO)_x]$ oxynitride support; Black, $Rh_{2-y}Cr_yO_3$ mixed oxide NP.

oxynitride does not evolve H_2 or O_2. The function of the $[(GaN)_{1-x}(ZnO)_x]$ oxynitride support is to absorb the photons, generate excited e^-/h^+ and supply the e^-/h^+ excitons to the photocatalytic active sites at the surface to perform the chemical reactions. It is thought that the function of the supported $Rh_{2-y}Cr_yO_3$ NPs is to selectively harness the electrons at its surface for H_2 evolution while the holes accumulate at the $[(GaN)_{1-x}(ZnO)_x]$ oxynitride surface to evolve O_2. The addition of $Rh_{2-y}Cr_yO_3$ NPs does not perturb the $[(GaN)_{1-x}(ZnO)_x]$ oxynitride bulk lattice characteristics (reflected by its same Raman spectrum and UV–vis band gap) or surface area indicating that the $Rh_{2-y}Cr_yO_3$ NPs are truly behaving as electronic promoters and are usually referred to as the cocatalyst. There are two ways to surface normalize the TOR_s: to the surface area of the $Rh_{2-y}Cr_yO_3$ NPs or to the overall surface area of the supported $Rh_{2-y}Cr_yO_3/[(GaN)_{1-x}(ZnO)_x]$ photocatalyst system, and both approaches will be examined below.

With modern cutting edge surface characterization techniques such as high sensitivity-low energy ion scattering (HS-LEIS), it is now also possible to directly quantify the number of surface Rh and Cr atoms on the outermost surface layer (~0.3 nm) of the photocatalyst. Given that Rh is well-known as an H_2 evolution promoter, the surface site normalized TOF photocatalytic reactivity will be normalized by the number of exposed Rh sites. The TOR_m, TOR_s, and TOF water splitting rates for several biphasic heterogeneous photocatalyst systems will be compared below.

Triphasic Heterogeneous Photocatalysts. Triphasic heterogeneous photocatalysts consist of three different phases and are exemplified by core–shell photocatalyst systems (e.g., supported $Cr_2O_3/Rh/[(GaN)_{1-x}(ZnO)_x]$,[15,16] $La_2O_3/Rh/[(GaN)_{1-x}(ZnO)_x]$,[17] etc.) for photocatalytic splitting of H_2O and is schematically depicted in Figure 3. In this triphasic photocatalyst, the metallic Rh core is initially photodeposited on the $[(GaN)_{1-x}(ZnO)_x]$ support, and the Cr_2O_3 shell is subsequently photodeposited on top of the metallic Rh core.[15,16] The motivation for this synthesis approach is to coat the metallic Rh sites to suppress the back reaction between H_2 and O_2 by metallic Rh to produce water as indicated in Figure 3. It is thought that the function of the metallic Rh core is to attract electrons that will tunnel through the Cr_2O_3 shell and react at the chromia surface with H^+ ions to evolve H_2 while the O_2 evolution takes place by reaction of the holes with H_2O at the surface of the $[(GaN)_{1-x}(ZnO)_x]$ oxynitride support. The addition of the Cr_2O_3/Rh core–shell NPs does not perturb the $[(GaN)_{1-x}(ZnO)_x]$ oxynitride bulk lattice characteristics (reflected by its same Raman spectrum and UV–vis band gap) or surface area indicating that the Cr_2O_3/Rh NPs truly behave as an electronic promoter, the cocatalyst, since the $[(GaN)_{1-x}(ZnO)_x]$ oxynitride support is not active for photocatalytic splitting of water. Similar to the biphasic heterogeneous photocatalyst systems discussed above, the TOR_m, TOR_s, and TOF water splitting rates for several triphasic heterogeneous photocatalyst systems will be compared below.

Comparison of Heterogeneous Photocatalysts for Splitting of Water. The performances of the above heterogeneous photocatalysts for water splitting are compared in Table 1 as PE, mass normalized reactivity (TOR_m), surface area normalized reactivity (TOR_s), and surface site normalized reactivity (TOF). For photocatalytic splitting of water, PE is defined by IUPAC[5] as

$$\mathrm{PE} = \frac{(\text{moles of } H_2 \text{ evolved}) \times 2 \times 100}{\text{moles of photons reaching the internal surface of the irradiation window}}$$

The factor of 2 in the above equation reflects that two photons are involved in forming one H_2 molecule. Although several excitations were employed for the various photocatalysts because of their different band gaps, comparing their performance for photocatalytic water splitting is still informative.

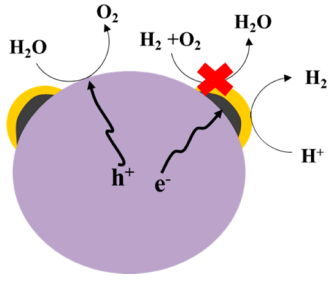

Figure 3. Schematic of triphasic heterogeneous photocatalysts for photocatalytic splitting of water. Purple, $[(GaN)_{1-x}(ZnO)_x]$ oxynitride support; Black, Rh metal core NP; Yellow, Cr_2O_3 shell.

The PE values are not available for all of the heterogeneous photocatalysts, but the reported PE values in Table 1 provide some important insights. The addition of only minor amounts of NiO to $NaTaO_3$-based photocatalysts with UV excitation gives rise to high PE values, as much as 56%, reflecting the electronic promoting characteristics of NiO for this photocatalyst system. In contrast, the best performing visible light activated supported $Rh_{2-y}Cr_yO_3/[(GaN)_{1-x}(ZnO)_x]$ photocatalyst only exhibits a PE value of 2.5%, a factor of ~20 lower, indicating the significant progress that is still needed to develop efficient water splitting heterogeneous photocatalysts. The impact of excitation source, UV vs visible, upon the photocatalytic splitting of water is also indicated in comparison of the supported $Rh_{2-y}Cr_yO_3/[(GaN)_{1-x}(ZnO)_x]$ photocatalyst at two different energies in Table 1. The TOR_m rate for the supported $Rh_{2-y}Cr_yO_3/[(GaN)_{1-x}(ZnO)_x]$ photocatalyst increases by a factor of ~15 in going from visible light excitation

dx.doi.org/10.1021/cs4005979 | ACS Catal. 2013, 3, 2606–2611

Table 1. Comparison of Heterogeneous Photocatalysts for Splitting of Water

photocatalyst	excitation source [nm (eV)]	BET [m^2/g]	PE [%]	TOR_m [H_2 μmol/g/h]	TOR_s [H_2 μmol/m^2/h]	TOR_s NPs[b] [H_2 μmol/m^2/h]	N_s [surface sites/g]	TOF [1/s]
TiO_2 (P-25)	>290 (4.3)	55		1.1×10^2[a]	2.0×10^0		2.8×10^{20}	6.7×10^{-5}
$NaTaO_3$[10]	>270 (4.6)	0.44		1.7×10^2	3.9×10^2			
0.05%NiO/$NaTaO_3$[10]	>270 (4.6)	0.44	28	2.2×10^3	5.0×10^3		1.2×10^{18}	3.0×10^{-1}
$NaTaO_3$: 2% La[10]	>270 (4.6)	3.2		4.5×10^2	1.4×10^2		1.3×10^{18}	5.8×10^{-2}
0.2%NiO/$NaTaO_3$: 2% La[10]	>270 (4.6)	3.2	56	2.0×10^4	6.2×10^3		4.8×10^{18}	6.8×10^{-1}
$Rh_{2-y}Cr_yO_3/[(GaN)_{1-x}(ZnO)_x]$20	>290 (4.3)	7.4		1.3×10^4	1.7×10^3	2.9×10^4	9.5×10^{17}	2.2×10^0
$Rh_{2-y}Cr_yO_3/[(GaN)_{1-x}(ZnO)_x]$[14]	>420 (2.95)	7.4	2.5	9.0×10^2	1.2×10^2	2.1×10^3	9.5×10^{17}	1.6×10^{-1}
$Cr_2O_3/Rh/[(GaN)_{1-x}(ZnO)_x]$[15]	>420 (2.95)	7.4	0.8	5.9×10^2	8.0×10^1	7.3×10^2	2.1×10^{18}	4.6×10^{-2}

[a]Initial rate. [b]NPs' surface area estimated from HS-LEIS.

(>420 nm) to UV excitation (>290 nm). The PE value for the supported $Rh_{2-y}Cr_yO_3/[(GaN)_{1-x}(ZnO)_x]$ photocatalyst under UV excitation has not been reported, but its PE value must be approaching that of the high performing UV activated NiO/$NaTaO_3$:La photocatalyst system since both photocatalysts exhibit comparable TOR_m values. The PE value is also strongly dependent on the structural arrangement of the Rh−Cr NPs on the $[(GaN)_{1-x}(ZnO)_x]$ support since with visible light activation the supported mixed oxide $Rh_{2-y}Cr_yO_3$ NPs exhibit a PE value of 2.5 while the supported core (Rh)/shell (Cr_2O_3) NPs have a PE value of 0.8 that is a factor of ∼3 lower.

The H_2 evolution TOR_m rates for most of the photocatalysts are comparable except for the most active 0.2% NiO/$NaTaO_3$:2%La UV-excited photocatalyst and most active visible light excited supported $Rh_{2-y}Cr_yO_3/[(GaN)_{1-x}(ZnO)_x]$ photocatalyst that are 1 to 2 orders of magnitude more active. These two most active photocatalysts exhibit comparable TOR_m rates when activated with UV radiation and, as already mentioned, changing from UV (>290 nm) to visible excitation (>420 nm) decreases the TOR_m rate by a factor of ∼15. The TiO_2 photocatalyst, which can only be activated with UV radiation because of its large band gap of ∼3.0−3.2 eV, however, is only able to evolve H_2 without concurrent production of O_2 and deactivates over time where the other photocatalysts are able to produce stoichiometric amounts of H_2 and O_2 and are stable with time. Under UV activation, the H_2 evolution TOR_m rate for NiO/$NaTaO_3$:La, the most active UV-activated catalyst, is ∼2 times higher than the TOR_m rate for $Rh_{2-y}Cr_yO_3/[(GaN)_{1-x}(ZnO)_x]$, the most active visible light activated photocatalyst. The slight increase between these two photocatalysts may be due to the greater excitation energy employed for NiO/$NaTaO_3$:La, > 270 nm, than for $Rh_{2-y}Cr_yO_3/[(GaN)_{1-x}(ZnO)_x]$, > 290 nm. The similar TOR_m rates for both of these highly effective catalysts under UV excitation indicate that photocatalysts optimized for visible light excitation can also perform efficiently under UV activation.

Additional fundamental insights are obtained when the H_2 evolution rates are surface area normalized (total surface area (TOR_s) or surface area of supported NPs (TOR_sNPs)) as already indicated above for the TiO_2 and $NaTaO_3$ photocatalyst system. Under UV activation, the TOR_s values for the photocatalysts vary by more than 3 orders of magnitude. The most investigated TiO_2 photocatalyst possesses the lowest surface area normalized photoactivity, which reflects the low activity rate of titania for photocatalytic splitting of water. Addition of La_2O_3 and NiO to $NaTaO_3$ have the opposite effects on the surface area normalized TOR_s rates with the former causing a slight decrease and the latter resulting in an order of magnitude increase. As already discussed above, La_2O_3 is a textural promoter that increases surface area and appears to suppress the specific photoactivity of $NaTaO_3$, while NiO is a potent electronic promoter. The most active surface area normalized photocatalyst under UV excitation is NiO/$NaTaO_3$:La reflecting the high concentration of photoactive surface sites for this photocatalyst system with a TOR_s rate that is ∼4 times greater than that for $Rh_{2-y}Cr_yO_3/[(GaN)_{1-x}(ZnO)_x]$, the most active visible light activated photocatalyst. The same surface areas for the mixed oxide $Rh_{2-y}Cr_yO_3/[(GaN)_{1-x}(ZnO)_x]$ and the core/shell Cr_2O_3/Rh/$[(GaN)_{1-x}(ZnO)_x]$ do not change their *relative* photoactivity values whether normalized by mass or surface area. Changing the excitation from UV to visible light decreases the TOR_s value by over an order of magnitude for $Rh_{2-y}Cr_yO_3/[(GaN)_{1-x}(ZnO)_x]$. Normalizing the photoactivity rates by the surface area of the Rh−Cr mixed oxide and core/shell NPs on the $[(GaN)_{1-x}(ZnO)_x]$ support, quantitatively determined with HS-LEIS surface analysis of the outermost surface layer, increase the TOR_s NPs rates by an order of magnitude due to the smaller surface area of the Rh−Cr NPs (0.4 and 0.8 m^2/g, respectively), and indicate that TOR_s NPs rate is ∼3 times greater for the Rh−Cr mixed oxide NPs than the Rh−Cr core/shell NPs. The above analysis demonstrates that a deeper fundamental understanding of the role of promoters (textural vs electronic) and concentration of photoactive surface sites for photocatalysts can be obtained when photocatalytic rates are also examined as TOR_s rates.

Analogous to reaction rate normalization practiced in heterogeneous catalysis,[7] the photocatalysis rates were also determined as TOF values and are reported in Table 1. Determination of TOF requires knowing the number of photoactive surface sites that are also given in Table 1. For TiO_2, the number of photoactive surface sites (N_s) was taken as the number density of surface titania sites. For the other photocatalysts, the N_s values were determined from HS-LEIS and HR-XPS surface analyses and are also indicated in Table 1. For the $NaTaO_3$:La photocatalyst, the photoactive surface sites are Ta and for the NiO/$NaTaO_3$:La, the photoactive sites become Ni because addition of the dispersed NiO increases the TOF by an order of magnitude. The number of photoactive surface sites per gram (N_s) is strongly related to the surface areas of the photocatalysts, $TiO_2 \gg Rh-Cr/[(GaN)_{1-x}(ZnO)_x] > NaTaO_3$:La > $NaTaO_3$, which suggests higher surface area photocatalysts that are activated by mildly energetic radiation (low band gap values) should be pursued in future studies to design advanced photocatalysts.

It is also important to emphasize the necessity to report surface analysis data for photocatalytic studies to ensure that heterogeneous photocatalysts are clean of surface impurities.

dx.doi.org/10.1021/cs4005979 | ACS Catal. 2013, 3, 2606−2611

For example, it was recently demonstrated that the high reactivity of nanocrystalline TiO_2 photocatalysts prepared with preferential exposure of the active (001) facet is actually related to contamination of the surface by F from the HF synthesis procedure that enhances the formation of the (001) facet.[18] Thus, it is critical to assess if synthesis methods or pretreatments produce a clean surface to ensure that the photocatalysis data are indeed representative of a clean photocatalytic system and are not being masked by the presence of extraneous surface impurities.[19]

Under UV activation, the TOF values vary from a low of 10^{-5} H_2 molecules/photoactive surface site/s to a high of ~2 × 10^0 H_2 molecules/photoactive surface site/s. TOF values of ~2 × 10^0/s are indeed impressive when compared to TOF values for thermally activated heterogeneous catalysis.[7] The lowest photoactivity TOF value is exhibited by TiO_2, the extremely low specific photoactivity rate of TiO_2 further indicates the rather low photoactivity of surface Ti sites relative to surface sites present on more advanced mixed oxide and oxynitride photocatalysts. The TOF photoactivity values for the UV-activated $NiO/NaTaO_3$ and $NiO/NaTaO_3$:La are comparable, only vary by ~2, further indicating that La_2O_3 is not an electronic promoter but is only a textural promoter that increases the overall surface area of the $NaTaO_3$ photocatalyst. The $NaTaO_3$ bulk UV−vis band gap is unperturbed by the introduction of NiO and La_2O_3, demonstrating that the promotion of NiO is only taking place in the surface region. The factor of ~2, if not associated with experimental error, may reflect the shorter distance that the excited e^-/h^+ must travel to reach the surface for the larger $NaTaO_3$ particles than the smaller $NaTaO_3$:La particles. The TOF values for the most active UV excited $NiO/NaTaO_3$/La photocatalyst is ~3 less compared to that of the most active visible light excited $Rh_{2-y}Cr_yO_3/[(GaN)_{1-x}(ZnO)_x]$ photocatalyst when activated with UV radiation. Changing the excitation light from UV (>290 nm) to the visible (>420 nm) range decreases the specific TOF by a factor of ~10 due to excitation with less energetic photons. Although the core/shell $Cr_2O_3/Rh/[(GaN)_{1-x}(ZnO)_x]$ has a greater number of surface Rh atoms than the mixed oxide $Rh_{2-y}Cr_yO_3/[(GaN)_{1-x}(ZnO)_x]$, the surface Rh sites on the core/shell photocatalyst possess a specific TOF value that is a factor of ~3 lower than the Rh sites on the mixed oxide photocatalyst, respectively. The lower specific photoactivity is most probably related to the presence of some surface Rh sites that are not covered by the Cr_2O_3 shell since unpromoted Rh will perform the reverse water oxidation reaction.[20] Determining the photocatalysis rates as TOF values have provided new fundamental insights about the specific rates for H_2 evolution per photoactive surface site and indicate that UV activated photocatalysts with rather impressive TOF values have already been discovered (1−2 H_2 molecules/photoactive surface site/s).

CONCLUSIONS

The above analyses of the series of photocatalysts for water splitting demonstrate that additional fundamental bulk and surface structural-photoactivity insights can be obtained by also determining photocatalysis rates as surface area normalized TOR_s and photoactive surface site normalized TOF than just the commonly accepted reporting of mass normalized TOR_m. The reporting of surface area normalized TOR_s values is critical to fundamentally understand the photocatalysis trends in a series of photocatalysts that are undergoing significant changes in surface area (e.g., series of TiO_2 and $NaTaO_3/NaTaO_3$:La). The reporting of N_s, from application of modern cutting edge surface analyses such as HS-LEIS and HR-XPS, provides new information about the number of photoactive surface sites (e.g., $Rh_{2-y}Cr_yO_3/[(GaN)_{1-x}(ZnO)_x]$ and $Cr_2O_3/Rh/[(GaN)_{1-x}(ZnO)_x]$) and specific photoactivity per photoactive surface site (e.g., comparable TOF values for UV activated $NiO/NaTaO_3$:La and $Rh_{2-y}Cr_yO_3/[(GaN)_{1-x}(ZnO)_x]$). Reporting of surface analysis of photocatalysts also needs to be adopted by the photocatalysis community since extraneous impurities from the synthesis may have a significant effect on the photoactivity and will only be known from application of surface analysis. It is proposed that the photocatalytic mass normalized TOR_m, surface area normalized TOR_s, and specific photoactive site normalized TOF rates, as well as PE values, be simultaneously reported in the photocatalysis literature because of the additional fundamental insights about the roles of the bulk lattice and surface features of photocatalysts that can be gained when reporting photocatalytic reactivity as PE, TOR_s, and TOF rates.

The challenges remaining for heterogeneous photocatalysis are to (*i*) increase the number density of photoactive surface sites, (*ii*) increase the specific photoactivity of the photoactive surface sites by at least an order of magnitude under visible light excitation, and (*iii*) discover materials with lower band gap values that will utilize a wider spectrum of the sun's light.

AUTHOR INFORMATION

Corresponding Author

*E-mail: iew0@lehigh.edu.

Present Address

[†](C.A.R.) Toyota Motor Engineering & Manufacturing North America, Inc., 1555 Woodridge Ave., Ann Arbor, Michigan 48105, United States

Notes

The authors declare no competing financial interest.

ACKNOWLEDGMENTS

The authors gratefully acknowledge the financial support by the Department of Energy- Basic Energy Sciences (Grant DOE-FG02-93ER14350). N. Sakamoto, Dr. K. Maeda, and Professor K. Domen at the University of Tokyo are thanked for assistance in obtaining the water splitting photocatalysis data for TiO_2.

REFERENCES

(1) Maschmeyer, T.; Che, M. *Angew. Chem., Int. Ed.* **2010**, *49*, 1536−1539.

(2) Maschmeyer, T.; Che, M. *Angew. Chem., Int. Ed.* **2010**, *49*, 9590−9591.

(3) Carneiro, J. T.; Savenije, T. J.; Moulijn, J. A.; Mul, G. *J. Phys. Chem. C* **2010**, *114*, 327−332.

(4) Carneiro, J. T.; Almeida, A. R.; Moulijn, J. A.; Mul, G. *Phys. Chem. Chem. Phys.* **2010**, *114*, 2744−2750.

(5) Braslavsky, S. E.; Braun, A. M.; Cassano, A. E.; Emeline, A. V.; Litter, M. I.; Palmisano, L.; Parmon, V. N.; Serpone, N. *Pure Appl. Chem.* **2011**, *83*, 931−1014.

(6) Serpone, N. *J. Photochem. Photobiol. A* **1997**, *104*, 1−12.

(7) Boudart, M.; Djéga-Mariadassou, G. *Kinetics of Heterogeneous Catalytic Reactions*; Princeton University Press: Princeton, NJ, 1984; p 222.

(8) Wang, C.; Zhang, Z.; Ying, J. Y. *Nanostruct. Mater.* **1997**, *9*, 583−586.

(9) Zhang, Z.; Wang, C.; Zakaria, R.; Ying, J. Y. *J. Phys. Chem. B* **1998**, *102*, 10871−10878.

(10) Kato, H.; Asakura, K.; Kudo, A. *J. Am. Chem. Soc.* **2003**, *125*, 3082−3089.
(11) Kudo, A.; Kato, H. *Chem. Phys. Lett.* **2000**, *331*, 373−377.
(12) Maruyama, M.; Iwase, A.; Kato, H.; Kudo, A.; Onishi, H. *J. Phys. Chem. C* **2009**, *113*, 13918−13923.
(13) Maeda, K.; Teramura, K.; Lu, D.; Takata, T.; Saito, N.; Inoue, Y.; Domen, K. *J. Phys. Chem. B* **2006**, *110*, 13753−13758.
(14) Maeda, K.; Teramura, K.; Domen, K. *J. Catal.* **2008**, *254*, 198−204.
(15) Maeda, K.; Teramura, K.; Lu, D.; Saito, N.; Inoue, Y.; Domen, K. *J. Phys. Chem. C* **2007**, *111*, 7554−7560.
(16) Maeda, K.; Teramura, K.; Lu, D.; Saito, N.; Inoue, Y.; Domen, K. *Angew. Chem., Int. Ed.* **2006**, *45*, 7806−7809.
(17) Yoshida, M.; Maeda, K.; Lu, D.; Kubota, J.; Domen, K. *J. Phys. Chem. C* **2013**, *117* (27), 14000−14006.
(18) Luan, Y.; Jing, L.; Xie, Y.; Sun, X.; Feng, Y.; Fu, H. *ACS Catal.* **2013**, *3*, 1378−1385.
(19) Yang, C.; Vernimmen, J.; Meynen, V.; Cool, P.; Mul, G. *J. Catal.* **2011**, *284*, 1−8.
(20) Maeda, K.; Teramura, K.; Saito, N.; Inoue, Y.; Domen, K. *J. Catal.* **2006**, *243*, 303−308.

dx.doi.org/10.1021/cs4005979 | *ACS Catal.* 2013, 3, 2606−2611